A Secure and Robust Frequency and Time Diversity Aided OFDM–DCSK Modulation System Not Requiring Channel State Information

Zhaofeng Liu, Lin Zhang, *Member, IEEE*, Zhiqiang Wu, *Senior Member, IEEE*, and Jing Bian

***Abstract*— In this paper, we propose a novel two-dimensional frequency and time diversity aided orthogonal frequency division multiplexing based differential chaos shift keying (OFDM-DCSK) system. Our aim is to provide secure and robust transmissions for practical wireless systems, where perfect channel state information (CSI) may not be available at the receiver, by exploiting the natural high security of chaotic sequences and frequency diversity gains brought by the frequency hopping (FH). In our design, the information bits are firstly modulated by chaotic chips, then non-repetitive FH operations are performed on both reference chips and chaotic modulated symbols. After the inverse fast Fourier transform (IFFT), the non-repetitive reference chips and chaotic modulated symbols are respectively transmitted over different subcarriers. Subsequently, the receiver recovers the information using the received reference chaotic chips which naturally embed the channel frequency response (CFR) of all subcarriers. We then analyze the energy and spectral efficiencies, derive the bit error rate (BER) and information leakage expressions, and provide a detailed complexity analysis of the proposed scheme. Simulation results verify the effectiveness of our derivations and demonstrate that the proposed system achieves better BER and security performances compared with the benchmark system, especially when the CSI is imperfect or unknown.**

***Index Terms*— Bit error rate, channel state information, differential chaos shift keying, two dimensional interleaving, security.**

I. Introduction

LIMITED radio frequency (RF) bandwidth has become a bottleneck for high data rate wireless communications. In order to meet the increasing demands for data rate of end users, carrier aggregation (CA) technology has been employed by the 3rd Generation Partnership Project (3GPP) Long Term Evolution-Advanced (LTE-A) to aggregate available bandwidth for transmissions [1], and cognitive radio (CR) technology is also utilized to identify available spectrum holes to allow the transmissions over unused or under-utilized subbands [2].

In CA or CR systems, the aggregated contiguous or non-contiguous frequency bands can provide more bandwidths. However, due to the possible discontinuity of specific bands, the receivers may not obtain accurate channel state information (CSI) estimation. Moreover, due to the broadcasting property of wireless channels, the CA and CR systems may suffer from eavesdropping or malicious attacks.

In order to enhance the security and robustness of wireless systems, chaotic communications have been widely used in some scenarios such as ultra-wide-band (UWB) communication and power line communication [3], [4] thanks to the natural high-security properties including non-periodicity, noise-like behavior, and sensitivity to initial value [5]. Chaotic communications include coherent chaotic modulations and non-coherent chaotic modulations, where non-coherent chaotic modulations have attracted more research interest due to the removal of complex chaotic synchronization circuits.

Among non-coherent chaotic modulation schemes, differential chaos shift keying [6] (DCSK) is considered more practical, since the DCSK receiver can be easily implemented and the bit error rate (BER) rate performance can meet the user demands [3] even when no channel estimation is available. The BER bounds for DCSK systems over multi-path fading channels have been derived in [7].

However, DCSK scheme has two main drawbacks. As mentioned in [3], one drawback is the low efficiency since the information-bearing symbols are delivered in only half of the DCSK symbol duration [8]–[10]. Another drawback is that the delay line used in the modulator is difficult to implement in practical circuits.

Recently, many research works have been done to improve the efficiency of the DCSK scheme by carrying more information bits via the information-bearing chaotic sequences [11]–[15], shortening the duration of chaos sequences [16], [17], or utilizing the index modulation [18] and spatial modulation [19]. Nevertheless, these methods still require delay line circuits, which is difficult to implement in practical systems. Therefore, multi-carrier (MC) transmission schemes have been applied in DCSK modulations [8] to improve the transmission

Manuscript received February 10, 2019; revised June 23, 2019, July 29, 2019, and October 11, 2019; accepted October 28, 2019. Date of publication November 5, 2019; date of current version March 18, 2020. This work was supported in part by the Project of National Natural Science Foundation of China under Grant 61602531, in part by Key Research and Development and Transformation Plan of Science and Technology Program for Tibet Autonomous Region (No. XZ201901-GB-16), in part by the NSF under Grant 1748494, and in part by the OFRN. The associate editor coordinating the review of this article and approving it for publication was T. Kim. *(Corresponding author: Lin Zhang.)*

Z. Liu and L. Zhang are with the School of Electronics and Information Technology, Sun Yat-sen University, Guangzhou 510006, China (e-mail: liuzhf5@mail2.sysu.edu.cn; isszl@mail.sysu.edu.cn).

Z. Wu is with the Department of Electrical Engineering, Tibet University, Lasa 850000, China, and also with the Department of Electrical Engineering, Wright State University, Dayton, OH 45435 USA (e-mail: zhiqiang.wu@wright.edu).

J. Bian is with the School of Data and Computer Science, Sun Yat-sen University, Guangzhou 510006, China (e-mail: mcsbj@mail.sysu.edu.cn).

Color versions of one or more of the figures in this article are available online at http://ieeexplore.ieee.org.

Digital Object Identifier 10.1109/TCOMM.2019.2951512

rate and remove the delay line, which is called MC-DCSK. Furthermore, the orthogonal frequency-division multiplexing (OFDM) technology, which allows the overlapping of multiple subcarriers orthogonal to each other and improves the bandwidth utilization efficiency of MC transmissions, has been combined with DCSK modulations to achieve higher data rate [9].

Although OFDM-DCSK systems can remove the delay line and increase the data rate via multi-carrier transmissions, they lost the inherent capability of DCSK to defend against frequency selective fading (FSF). In [20], [21], DCSK systems have been verified that they can achieve satisfactory BER performances over frequency selective Rayleigh fading channel without CSI, thanks to the high auto-correlation and low cross-correlation values among chaotic sequences [22], [23]. However, this property can not be retained due to the cross-correlation existing among the OFDM-DCSK symbols, thus the OFDM-DCSK systems can not work well over FSF channels.

In order to improve the performance to combat the FSF, [24] has proposed to apply the Walsh code sequences to achieve the orthogonality of the reference signal and the information signal in the code domain. However, due to the FSF, the orthogonality can be hardly well maintained at the receiver, thereby degrading the BER performances. On the other hand, the frequency domain equalizer (FDE) [25] has been widely used to combat the FSF with the low complexity. However, they require to know the exact CSI to accomplish the FDE over FSF channels [26]. Especially in CA or CR systems which aggregate non-contiguous bands, the FSF across the non-contiguous bands brings a significant challenge since the exact CSI estimates become even more difficult to obtain.

In addition, OFDM-DCSK systems inherit the defect of the DCSK modulation, i.e., they have lower security performances due to the direct transmission of the reference chaotic sequences [27]. Recently, researchers have proposed to enhance the security performances of the DCSK systems by scrambling the chaotic chips [15], [28]–[31]. However, these schemes scramble the chaotic chips in the time domain so delay line circuits are still required. Similar work has been done whereas the chaotic chips are scrambled in the frequency domain [32]. Unfortunately, in [32], only half of the spectrum is exploited to transmit the information-bearing symbols, which degrades the spectrum efficiency. The major two drawbacks of delay line implementation and low spectrum efficiency are still not fully addressed.

To enhance secure and robust transmissions for end users in CA or CR systems operating over non-contiguous bands, which may have to utilize imperfect CSI, we propose to utilize the natural high security properties of chaotic sequences, including sensitivity to initial value and non-periodicity [5], and the diversity gain brought by frequency hopping (FH).

In this paper, we propose a secure and robust frequency-and-time hybrid-interleaving OFDM-DCSK (FH-OFDM-DCSK) modulation scheme not requiring CSI. Different from conventional OFDM-DCSK systems, the hopping scheme is used to distribute chaotic chips of chaotic sequences to different subcarriers and different time slots before inverse fast Fourier transform (IFFT) at the transmitter. Instead of focusing on improving the data rate, our design aims to improve the security and robustness of DCSK systems, especially when the information is transmitted over channels having various channel conditions or the CSI may not be obtained at receivers.

Specifically, at the transmitter, after the serial to parallel (S/P) conversion, the information is modulated by chaotic chips. Then the reference chaotic chips and the chaotic modulated symbols randomly hop in different time slots and over different subcarriers. After the hopping, all chaotic chips of one chaotic sequence are respectively distributed over different subcarriers. Thus the CFR over each subcarrier will be naturally embedded into the transmitted signals. At the receiver, correlation demodulation is performed on different sequences. Thanks to the CFR embedded in the received signals over each subcarrier, the demodulation can recover the signals more reliably by counteracting the CFR and utilizing the frequency diversity gain even when no CSI estimates are provided. By contrast, although similar frequency diversity gain can be achieved by combing time interleaving and code division multi-access (CDMA) schemes [33], without known CSI, these systems cannot work well over channels with different channel conditions. Thanks to the FH operations, our proposed design can provide enhanced robustness performances when operating over different types of channels. In addition, the proposed FH aided OFDM-DCSK method can provide an extra benefit that no additional correlation module is added, which means that our design could be easily integrated with practical systems. Moreover, only the legitimate receivers with known hopping pattern can retrieve the information, therefore the security performances are also improved.

The main contributions of this paper include:

1) We present a frequency and time diversity aided OFDM-DCSK scheme to improve both the security and the BER performances. No perfect CSI is required for information recovery at the receiver. The information can be retrieved at the receiver by utilizing the high auto-correlation value and low cross-correlation value of chaotic sequences.
2) The proposed FH-OFDM-DCSK scheme can work well in CA or CR systems over non-contiguous bands. Thanks to the frequency diversity gain, better BER performances can be achieved especially when transmitted over FSF channels or no perfect CSI can be obtained.
3) We enhance the security performances by scrambling both the chaotic chips and the information-bearing chaotic modulated symbols. The correlations among different OFDM symbols are weakened and the security performances are improved.
4) We analyze the theoretical efficiency, reliability and security performances, as well as computational complexity. We compare the energy and spectral efficiencies of the proposed system with counterpart systems. Then we derive the theoretical BER expressions over additive white Gaussian noise (AWGN) channel, slow flat fading channel and independently and identically distributed (i.i.d.) frequency selective Rayleigh fading channel. Subsequently, we provide information leakage expressions

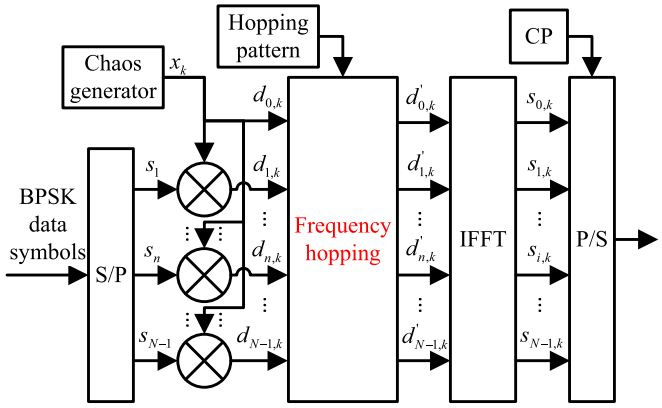

Fig. 1. The FH-OFDM-DCSK transmitter structure.

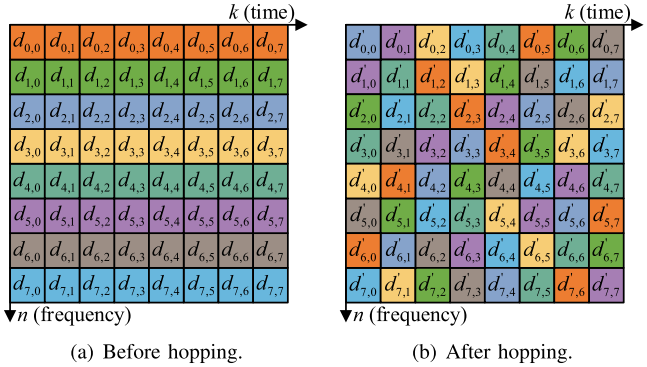

(a) Before hopping. (b) After hopping.

Fig. 2. Illustration of the distributions of chaotic symbols in the time domain and the frequency domain before and after the frequency hopping. $N = 8$ and $\beta = 8$.

for security analysis and compare the complexity of the proposed system with that of counterpart systems. Numerical simulations are performed to demonstrate the outstanding performances of the proposed scheme compared with counterpart schemes.

The rest of the paper is organized as follows: the FH-OFDM-DCSK design is proposed in Section II, Section III provides the theoretical BER analysis over i.i.d. frequency selective Rayleigh fading channel and security analysis. Simulation results are provided in Section IV to verify the improvement of BER and security performances. Finally, we conclude the paper in Section V.

II. The FH-OFDM-DCSK Design

In this section, we provide the details of the proposed FH-OFDM-DCSK scheme, including the transceiver structure, hopping and de-hopping modules.

A. FH-OFDM-DCSK Transmitter Structure

Fig. 1 illustrates the proposed FH-OFDM-DCSK transmitter. The user data are firstly modulated by binary phase shift keying (BPSK) scheme, then after serial to parallel (S/P) conversion, the BPSK data symbols are modulated by the chaotic sequences generated by the chaos generator. Subsequently, both the reference chaotic chips and the chaotic modulated symbols hop randomly in the frequency domain via the frequency hopping module. The resultant symbols are then fed to the IFFT module to construct the OFDM symbols. After adding the cyclic prefix (CP) and parallel to serial (P/S) conversions, these symbols are transmitted over the channels.

Specifically, in the chaos generator, we employ the second order Chebyshev polynomial function (CPF) to generate the chaotic sequences of length β. Namely, the reference chaotic sequence is generated by $x_{k+1} = 1 - 2x_k^2$ and $0 \leq k \leq \beta - 1$, where x_k denotes the kth chip of the chaotic sequence.

The resultant reference chaotic sequences are then used to modulate user data, followed by the frequency hopping and IFFT operations to be detailed as below.

1) Chaotic Modulation: Let s_n denote the nth ($n = 1, 2, \ldots, N-1$) BPSK data symbol. We modulate the s_n with the kth chaotic chip, the resultant information-bearing chaotic modulated symbol $d_{n,k}$ is expressed as

$$d_{n,k} = s_n x_k. \tag{1}$$

Notably, for the sake of brevity to express the data input to the frequency hopping module, we here set $n = 0, 1, \ldots, N-1$ for $d_{n,k}$ and $d_{0,k} = x_k$ to include the case that there is one sub-channel which is required to transmit the reference chaotic chip. More explicitly, when $n = 0$, $d_{0,k}$ denotes the kth reference chaotic chip, while when $1 \leq n \leq N-1$, $d_{n,k}$ denotes the information bearing chaotic chips $d_{n,k} = s_n x_k$.

Then the elements of $d_{n,k}$ with all n and k are sent to the frequency hopping module and hop randomly in the frequency domain as follows.

2) Frequency Hopping: In the frequency hopping module, the input symbols $d_{n,k}$ hop randomly and non-repetitively, then we obtain the output symbols denoted by $d'_{n,k}$ under the assumption that the length of the chaotic sequence equals to the subcarrier number, i.e., $\beta = N$.

Fig. 2 illustrates the distributions of the reference chaotic chips and the information-bearing chaotic modulated chips in the time domain and frequency domain before and after the frequency hopping when $\beta = N = 8$. In Fig. 2, each color block refers to one chip of chaotic sequences, and blocks of different color correspond to different chaotic sequences. The chaotic chips shown in Fig. 2(a) hop at different frequencies non-repetitively to combat the frequency selective fading. In addition, as illustrated by Fig. 2(b), they are also interleaved in different time slots to weaken the correlations among OFDM symbols to improve the reliability and security performances. Therefore, with the frequency hopping in the frequency domain and the interleaving in the time domain, the chaotic chips exchange non-repetitively and thus the index of the subcarrier and the index of the time slot for a specific chaotic chip will change accordingly.

Next, we derive the frequency hopping matrix to analytically express the hopping operations. We define the frequency hopping operation as a matrix denoted by $\mathbf{U}$ and assume $\beta = N$.

Firstly, the chips are collected in every β time slots before the hopping operation. The matrix constructed by

Algorithm 1 Generating g_k

Input: $\mathbf{c_m}$
Output: g_k
Initialization :
$g_k = 0$
LOOP Process
for $q = 0$ to $\beta - 1$ **do**
  if $(c_{m,k} > c_{m,q})$ **then**
    $g_k = g_k + 1$
  end if
end for
return g_k

the input chips are denoted by $\mathbf{D} = [\mathbf{d_0}^T, \mathbf{d_1}^T, \ldots, \mathbf{d_k}^T, \ldots, \mathbf{d_{\beta-1}}^T]$, where $(\cdot)^T$ denotes the transposition and $\mathbf{d_k} = [d_{0,k}, d_{1,k}, \ldots, d_{n,k}, \ldots, d_{N-1,k}]$.

Then the frequency hopping operations can be expressed as [34]

$$\mathbf{d'_n} = \mathbf{d_k}\mathbf{U_k} \tag{2}$$

where $\mathbf{U_k}$ denotes the hopping matrix corresponding to the kth chaotic sequence $\mathbf{d_k}$, $n = k$, which determines the hopping pattern, $\mathbf{d'_n} = [d'_{n,0}, d'_{n,1}, \ldots, d'_{n,k}, \ldots, d'_{n,\beta-1}]$ is the nth chaotic sequence which constitutes $\mathbf{D'} = [\mathbf{d'_0}^T, \mathbf{d'_1}^T, \ldots, \mathbf{d'_n}^T, \ldots, \mathbf{d'_{N-1}}^T]^T$.

Notably, in the hopping matrix $\mathbf{U_k}$, there is only one "1" in each row and each column. When the random hopping pattern is employed, the position of the element "1" will be randomly distributed. Meanwhile, $\mathbf{U_k}$ has the constraint that the result of $\sum_{k=0}^{\beta-1} \mathbf{U_k}$ is the matrix whose all elements are "1". For example, in the case that the cyclic hopping pattern is employed, then according to [34], $\mathbf{U_k}$ is defined as

$$\mathbf{U_k} = \begin{bmatrix} \mathbf{0} & \mathbf{E_{g_k}} \\ \mathbf{E_{N-g_k}} & \mathbf{0} \end{bmatrix} \tag{3}$$

where $\mathbf{E_{g_k}}$ is the $g_k \times g_k$-dimension identity matrix and $\mathbf{E_{N-g_k}}$ is the $(N-g_k)\times(N-g_k)$-dimension identity matrix.

In order to enhance the security performance, we here propose to further hide the hopping pattern by exploiting the aperiodicity property of the chaotic sequence. As suggested by our previous work in [35], we can generate the dimension g_k in Eq. (3) using the chaotic scrambling method. Namely, let $\mathbf{c_m} = [c_{m,0}, c_{m,1}, \ldots, c_{m,N-1}]$ denote the chaotic sequence used to determine the hopping pattern. Then g_k can be generated with $\mathbf{c_m}$ according to Algorithm 1.

In general, no matter what the hopping pattern is, for each chip in the chaotic sequence, we can rewrite the frequency hopping operations based on Eq. (2) as

$$d_{n,k} = d'_{k,f(n,k)} \tag{4}$$

where $f(n,k)$ determines the hopping pattern. Take the cyclic hopping pattern as an example, for the nth chaotic modulated symbol and the kth chaotic chip, $f(n,k)$ can be written as $f(n,k) = (n + g_k) \mod \beta$, where mod is the modulo operation.

From Eq. (2)-Eq. (4), we can see that the frequency hopping module guarantees that the chaotic chips from all chaotic sequences over each subcarrier are transmitted in different and random time slots. Therefore, when we transmit user data over FSF channels, the frequency diversity can be exploited for the information reception and different CFR of every subcarrier can be figured out. In addition, the randomness of OFDM symbols is enhanced and the cross-correlation of different OFDM symbols is weakened. Thus, except for the benefit of the enhance security performance, the hopping in both the frequency domain and the time domain will enhance the robustness of the OFDM-DCSK schemes.

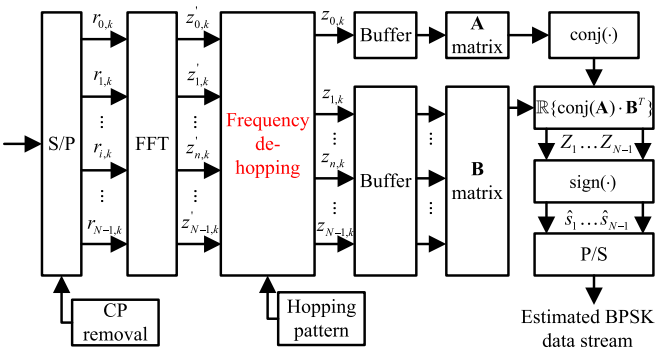

Fig. 3. The FH-OFDM-DCSK receiver structure.

In the general case of $N \neq \beta$, the chaotic chips can be distributed in a way similar to the hopping pattern shown in Fig. 2. The reason is that in most cases the number of available subcarriers N can be known by the transceiver, thus the length of chaotic sequences β can be adjusted accordingly. For example, if the transceiver sets $N = \gamma\beta$ where γ is an integer, the shape of the hopping pattern is rectangular. Therefore, the hopping pattern can be split into γ square sub-hopping patterns and each sub hopping-pattern can be generated according to Fig. 2.

3) OFDM Modulation: After the frequency hopping, the IFFT operations are performed on $d'_{n,k}$ as below

$$s_{i,k} = \frac{1}{\sqrt{N}} \sum_{n=0}^{N-1} d'_{n,k} e^{j\frac{2\pi n i}{N}} \tag{5}$$

where N is the number of subcarriers, k is the index of chaotic chip time slot, i is the index of the IFFT-modulated symbols in a chip time slot, n is the index of the subcarrier. Then the resultant OFDM symbols are transmitted over the channels after P/S conversion and adding CP.

B. FH-OFDM-DCSK Receiver Structure

Fig. 3 illustrates the FH-OFDM-DCSK receiver. After the serial to parallel conversion and CP removal, the received data symbols are sent to the fast Fourier transform (FFT) module to perform OFDM demodulation. Notably, after the FFT transform, we obtain the signals in the frequency domain. Then the OFDM-demodulated symbols are delivered to the frequency de-hopping module to recover the original chaotic modulated symbols sequentially. The de-hopped symbols are saved in buffers and sequentially chosen in every β symbols to perform the correlation demodulation. Namely, the resultant OFDM demodulated bits in the frequency domain are recovered by de-spreading the correlation of the received reference

sub-carrier signal and information bearing sub-carrier signals. It is noticeable that the bit recovery operations are performed in the frequency domain, i.e. the subcarrier domain. Finally, the maximum likelihood detection is applied to estimate information symbols. More detailed descriptions about the information recovery operations carried out in the legitimate receivers are proposed as below.

1) OFDM Demodulation: At the receiver, after the FFT, the received symbol $z'_{n,k}$ over the nth subcarrier corresponding to the kth chaotic chip is denoted by

$$z'_{n,k} = \frac{1}{\sqrt{N}} \sum_{i=0}^{N-1} r_{i,k} e^{-j\frac{2\pi ni}{N}} = H_{n,k} d'_{n,k} + \xi_{n,k} \tag{6}$$

where $r_{i,k}$ denotes the received data symbol over the nth subcarrier corresponding to the ith chaotic chip, $\xi_{n,k} = \rho_{n,k} + j\iota_{n,k}$ is the complex Gaussian noise with zero mean and power spectral density of N_0 so that $\mathrm{E}\{|\xi_{n,k}|^2\} = 2\mathrm{E}\{\rho^2_{n,k}\} = 2\mathrm{E}\{\iota^2_{n,k}\} = N_0$, $H_{n,k}$ is the actual CFR over the nth subcarrier corresponding to the kth OFDM symbol. To elaborate a bit further, if the channel undergoes the slow fading, then the CFRs across different OFDM symbols remain almost the same, while for flat fading channels, the CFRs across different subcarriers are also approximately identical. For the brevity of expressions, for slow fading channels, $H_{n,k}$ remains almost the same for all chaotic chip index $k \in [0, \beta - 1]$ and k could be omitted. Similarly, for flat fading channels, $H_{n,k}$ remains almost the same for all the subcarrier index $n \in [0, N-1]$ and we could use H_k to represent the time-varying channel condition for conciseness.

2) Frequency De-Hopping: Next, the frequency de-hopping operations are performed on the OFDM demodulated symbols. For the legitimate receivers, before the transmission of the user data, the de-hopping pattern is delivered via the specific control channel or via secure uncoordinate transmissions [36], [37]. For instance, in the proposed FH-OFDM-DCSK system, we apply the uncoordinate direct sequence spread spectrum (UDSSS) technique proposed in [36] to transmit the secret de-hopping pattern. To elaborate a bit further, in the UDSSS aided FH-OFDM-DCSK system, firstly we generate a set of chaotic sequences $\mathcal{C}$, then we randomly choose the chaotic sequence $\mathbf{c_m}$ used to generate the hopping pattern according to Algorithm 1. At the receiver, the buffer will be used to collect chaotic chips, then the chips will be de-hopped by the chaotic sequences in $\mathcal{C}$ with a trial-and-error approach [36]. Subsequently, we evaluate the correlations between different de-hopped chaotic sequences, and select the most probable chaotic sequence $\mathbf{c}^*_\mathbf{m}$ in $\mathcal{C}$. At last, the de-hopping pattern can be determined by $\mathbf{c}^*_\mathbf{m}$, which will be further used for de-hopping operations.

Considering the assumptions that $\beta = N$ at the transmitter, similar to Eq. (2), given $\mathbf{Z}' = [\mathbf{z'_0}^T, \mathbf{z'_1}^T, \ldots, \mathbf{z'_n}^T, \ldots, \mathbf{z'_{N-1}}^T]^T$ and $\mathbf{z'_n} = [z'_{n,0}, z'_{n,1}, \ldots, z'_{n,k}, \ldots, z'_{n,\beta-1}]$, in the case that the cyclic hopping pattern is employed, the frequency de-hopping can be derived as

$$\mathbf{z_k} = \mathbf{z'_n} {\mathbf{U_k}}^{-1} \tag{7}$$

where $n = k$, ${\mathbf{U_k}}^{-1}$ is the inverse matrix of $\mathbf{U_k}$, the resultant vector after the de-hopping operations is $\mathbf{z_k} = [z_{0,k}, z_{1,k}, \ldots, z_{n,k}, \ldots, z_{N-1,k}]$ and $\mathbf{Z} = [\mathbf{z_0}^T, \mathbf{z_1}^T, \ldots, \mathbf{z_k}^T, \ldots, \mathbf{z}^T_{\beta-1}]$.

Besides cyclic hopping pattern, we can also use other hopping patterns such as the random hopping pattern. In this case, the de-hopping operations are determined by

$$z_{n,k} = z'_{k,f(n,k)} \tag{8}$$

where $f(n,k)$ has the same expression as the one given above, i.e. $f(n,k) = (n + g_k) \bmod \beta$, wherein g_k is determined by Algorithm 1.

By contrast, the eavesdropper cannot eavesdrop the information without the knowledge of hopping matrix $\mathbf{U_k}$ used in the transmitter.

3) Detection and Estimation: After the frequency de-hopping, the obtained reference chaotic chips from different chaotic sequences are stored in buffers. Next, the correlated demodulations are performed on the reference chaotic sequence and information bearing chaotic sequences, then we can obtain the nth information symbol by calculating

$$Z_n = \Re \left\{ \sum_{k=0}^{\beta-1} \mathrm{conj}(z_{0,k}) \cdot z_{n,k} \right\} \tag{9}$$

where $\Re\{\cdot\}$ takes the real part of signal, $\mathrm{conj}(\cdot)$ represents the conjugate operation and $z_{0,k}$ is the kth element of the reference chaotic sequence.

Finally, we perform the maximum likelihood detection for received symbols, the resultant estimates $\hat{s}_n$ of BPSK modulated symbols can be obtained as $\hat{s}_n = \mathrm{sgn}(Z_n)$, where $\mathrm{sgn}(\cdot)$ is the sign function.

Notably, it can be seen from Eq. (9) that no CSI estimates are required for the information retrieval. Hence with our FH-OFDM-DCSK design, we can recover the information by utilizing the frequency diversity and the ergodic property of wireless channels, which means that the proposed FH-OFDM-DCSK scheme can effectively combat the FSF and enhance the robustness performances of OFDM-DCSK systems, which would be verified via following theoretical analysis and simulation results.

III. Performance Analysis

In this section, we will analyze and compare the efficiency, reliability and security performances and evaluate the complexity of the proposed FH-OFDM-DCSK system with the benchmark OFDM-DCSK system [9], which also acts as the benchmark scheme in [10], and the OFDM code shifted DCSK (OFDM-CS-DCSK) system [24]. For fairness of comparisons, since the original OFDM-DCSK system is presented for AWGN channel, here we propose to add a FDE module to enhance the performances, which is named as the FDE-aided OFDM-DCSK scheme (FDE-OFDM-DCSK) [9], [25].

A. Energy Efficiency and Spectral Efficiency

1) Energy Efficiency: The energy efficiency is defined as the data-energy-to-bit-energy-ratio (DBR) [10]. Let E_{data}, $E_{ref}$and E_b respectively represent the energy of data, chaotic sequences and bits, we have $DBR = E_{data}/E_b$.

For OFDM-DCSK systems, neglecting the energy cost of CP symbols, E_b can be calculated with E_{data} and E_{ref}. For example, similar to the FDE-OFDM-DCSK system, in the proposed FH-OFDM-DCSK system, $N-1$ bits share one reference chaotic sequence, hence we have $E_b = E_{data} + E_{ref}/(N-1)$ [10], where $E_{data} = E_{ref} = T_c \sum_{k=0}^{\beta-1} x_k^2$ and T_c denotes the duration of one chaotic chip. Then the energy efficiency can be obtained as $DBR = (N-1)/N$. Similarly, for the OFDM-CS-DCSK system [24], we can also derive the DBR as $(N-1)/N$.

From the above analysis, we can see that the proposed FH-OFDM-DCSK system has the same energy efficiency as that of system FDE-OFDM-DCSK and OFDM-CS-DCSK system [24].

2) Spectral Efficiency: The spectral efficiency can be measured by the number of bits transmitted per OFDM-DCSK symbol. Let T_{OFDM} denote the duration of one OFDM symbol, and B denote the occupied bandwidth of one OFDM symbol, then for FDE-OFDM-DCSK system, $N-1$ bits will be transmitted with β OFDM symbols, thus the spectral efficiency of FDE-OFDM-DCSK system is $(N-1)/(B\beta T_{OFDM})$. As to our proposed FH-OFDM-DCSK system, the FH operations will not induce additional bits or chaotic chips for transmissions, hence the spectral efficiency will remain the same as that of FDE-OFDM-DCSK system. For OFDM-CS-DCSK systems [24], for fairness of comparisons, the interval of subcarriers are set as the same as the other two systems. The occupied bandwidth is NB, the duration is T_{OFDM} and the number of transmitted bits is $N-1$, thus the spectral efficiency is also $(N-1)/(B\beta T_{OFDM})$.

Based on the spectral efficiency analysis, we can conclude that the proposed FH-OFDM-DCSK system has the same energy efficiency as that of the FDE-OFDM-DCSK system and the OFDM-CS-DCSK system [24].

B. BER Performance

In this subsection, we assume that β is large enough, thus we employ the Gaussian approximation (GA) method [7] to derive the theoretical BER expressions over wireless channels, including the additional white Gaussian noise (AWGN) channel, slow flat fading channel, and slow i.i.d. frequency selective Rayleigh fading channel. That is to say, we assume that additive noises exist in the channel, and the channel coherent time is larger than the symbol duration, thus the channels undergo the slow fading. Namely, the channels remain time-invariant in the whole OFDM-DCSK symbol duration including β OFDM durations. Besides, different subcarriers may have different CFR due to the i.i.d. FSF assumptions.

1) BER for Legitimate Users: Firstly, we derive the received de-hopped symbols by using Eq. (4), Eq. (6) and Eq. (8) as

$$\begin{aligned} z'_{k,f(n,k)} &= z_{n,k} = H_{k,f(n,k)} d'_{k,f(n,k)} + \xi_{k,f(n,k)} \\ &= H_k d_{n,k} + \xi_{k,f(n,k)} \end{aligned} \tag{10}$$

where $z_{0,k}$ denotes the reference chaotic chip corresponding to $n=0$, when $n \geq 1$, $z_{n,k}$ is the information-bearing modulated chip. $H_{k,f(n,k)}$ represents the CFR of the subchannel corresponding to the kth subcarrier transmitting the $f(n,k)$th OFDM symbol. As mentioned above, for slow fading channels, $H_{k,f(n,k)}$ are time invariant in the OFDM-DCSK symbol duration. For the sake of brevity, we here omit the symbol index $f(n,k)$, and use H_k to represent the CFR of the kth subchannel, which remains the same for β OFDM symbols which constitute one OFDM-DCSK symbol. $\xi_{k,f(n,k)}$ is the noise obtained after hopping operations are carried out with the same mean and variance as $\xi_{n,k}$.

Then, from Eq. (9) and Eq. (10), we can derive the demodulated symbol Z_n for $n \geq 1$ as

$$\begin{aligned} Z_n &= \Re\left\{\sum_{k=0}^{\beta-1} \mathrm{conj}\left(z_{0,k}\right) \cdot z_{n,k}\right\} \\ &= \Re\left\{\sum_{k=0}^{\beta-1} \mathrm{conj}\left(z'_{k,f(0,k)}\right) z_{k,f(n,k)}\right\} \\ &= \Re\Bigg\{\sum_{k=0}^{\beta-1} \left(H_{k,f(0,k)} d'_{k,f(0,k)} + \xi_{k,f(0,k)}\right)^* \\ &\qquad \left(H_{k,f(n,k)} d'_{k,f(n,k)} + \xi_{k,f(n,k)}\right)\Bigg\}. \end{aligned} \tag{11}$$

For slow fading channels, we omit the symbol index $f(0,k)$ and $f(n,k)$ in $H_{k,f(0,k)}$ and $H_{k,f(n,k)}$, then Eq. (11) becomes

$$\begin{aligned} Z_n &= \Re\left\{\sum_{k=0}^{\beta-1} (H_k d_{0,k} + \xi_{k,f(0,k)})^* (H_k d_{n,k} + \xi_{k,f(n,k)})\right\} \\ &= \underbrace{\Re\left\{\sum_{k=0}^{\beta-1} s_n |H_k|^2 x_k^2\right\}}_{P_1} + \underbrace{\Re\left\{\sum_{k=0}^{\beta-1} \xi^*_{k,f(0,k)} \xi_{k,f(n,k)}\right\}}_{P_2} \\ &\quad + \underbrace{\Re\left\{\sum_{k=0}^{\beta-1} (H^*_k x_k \xi_{k,f(n,k)} + s_n H_k x_k \xi^*_{k,f(0,k)})\right\}}_{P_3} \end{aligned} \tag{12}$$

where $(\cdot)^*$ represents the conjugation operation, P_1 contains the desired signal, while P_2 and P_3 are the disturbance components. Since P_1, P_2 and P_3 are statistically independent, the expectation and variance of Z_n can be easily calculated by

$$\begin{aligned} \mathrm{E}\{Z_n|(s_n = \pm 1)\} &= \sum\nolimits_{w=1}^{3} \mathrm{E}\{P_w|(s_n = \pm 1)\} \\ \mathrm{var}\{Z_n|(s_n = \pm 1)\} &= \sum\nolimits_{w=1}^{3} \mathrm{var}\{P_w|(s_n = \pm 1)\} \end{aligned} \tag{13}$$

where $\mathrm{E}\{\cdot\}$ denotes the expectation operator and $\mathrm{var}\{\cdot\}$ represents the variances. Then we could obtain the signal-to-noise-plus-interference ratio (SINR) expression as

$$\Gamma = \frac{(\mathrm{E}\{Z_n|(s_n = \pm 1\})^2}{\mathrm{var}\{Z_n|(s_n = \pm 1\}}. \tag{14}$$

We further derive the statistical characteristics of P_1, P_2 and P_3 using the central limit theorem as below

$$\begin{aligned} &\mathrm{E}\{P_1|s_n = +1\} = -\mathrm{E}\{P_1|s_n = -1\} \\ &\quad = \sum_{k=0}^{\beta-1} \mathrm{E}\left\{|H_k|^2\right\} \mathrm{E}\left\{x_k^2\right\} = \beta \mathrm{E}\left\{|H_k|^2\right\} \mathrm{E}\left\{x_k^2\right\} \end{aligned} \tag{15a}$$

$$\mathrm{E}\{P_2|s_n = \pm 1\} = \mathrm{E}\{P_3|s_n = \pm 1\} = 0 \tag{15b}$$

$$\begin{aligned}\mathrm{var}\{P_1|s_n=\pm1\}&=\beta\mathrm{var}\left\{|H_k|^2x_k^2\right\}\\&=\beta\left(\mathrm{E}\left\{|H_k|^4\right\}\mathrm{E}\left\{x_k^4\right\}-\mathrm{E}\left\{|H_k|^2\right\}^2\mathrm{E}\left\{x_k^2\right\}^2\right)\end{aligned}\tag{15c}$$

$$\begin{aligned}\mathrm{var}\{P_2|s_n=\pm1\}&=\beta\mathrm{var}\left\{\Re\left\{\xi^*_{k,f(0,k)}\xi_{k,f(n,k)}\right\}\right\}\\&=\beta\left(\mathrm{var}\left\{\rho_{k,f(0,k)}\rho_{k,f(n,k)}\right\}+\mathrm{var}\left\{\iota_{k,f(0,k)}\iota_{k,f(n,k)}\right\}\right)\\&=2\beta\cdot\frac{N_0}{2}\cdot\frac{N_0}{2}=\frac{1}{2}\beta N_0^2\end{aligned}\tag{15d}$$

$$\begin{aligned}&\mathrm{var}\{P_3|s_n=\pm1\}\\&=\beta\mathrm{var}\left\{\Re\left\{H_k^*x_k\xi_{k,f(n,k)}+s_nH_kx_k\xi^*_{k,f(0,k)}\right\}\right\}\\&=\beta\mathrm{var}\big\{H_{rk}x_k\rho_{k,f(n,k)}+H_{ik}x_k\iota_{k,f(n,k)}\\&\quad+H_{rk}x_k\rho_{k,f(0,k)}+H_{ik}x_k\iota_{k,f(0,k)}\big\}\\&=\beta\Big(\mathrm{E}\left\{H_{rk}^2x_k^2\rho^2_{k,f(n,k)}\right\}+\mathrm{E}\left\{H_{ik}^2x_k^2\iota^2_{k,f(n,k)}\right\}\\&\quad+\mathrm{E}\left\{H_{rk}^2x_k^2\rho^2_{k,f(0,k)}\right\}+\mathrm{E}\left\{H_{ik}^2x_k^2\iota^2_{k,f(0,k)}\right\}\Big)\\&=\beta\mathrm{E}\left\{|H_k|^2\right\}\mathrm{E}\{x_k^2\}N_0.\end{aligned}\tag{15e}$$

For the slow and FSF channel, the BER of the proposed FH-OFDM-DCSK system can be derived as

$$\begin{aligned}BER_{selective}&=\frac{1}{2}\mathrm{erfc}\left(\sqrt{\frac{\Gamma}{2}}\right)\\&=\frac{1}{2}\mathrm{erfc}\left[\left(\frac{2\mathrm{var}\{Z_n|(s_n=\pm1)\}}{\mathrm{E}\{Z_n|(s_n=\pm1)\}^2}\right)^{-\frac{1}{2}}\right]\end{aligned}\tag{16}$$

where $\mathrm{var}\{Z_n|(s_n=\pm1)\}$ and $\mathrm{E}\{Z_n|(s_n=\pm1)\}^2$ can be calculated based on Eq. (13) and Eq. (15). From Eq. (16), we can observe that the BER of FH-OFDM-DCSK is dependent on the higher-order statistics of x_k and $|H_k|$. The chaos sequences generated by CPF have the property that $\mathrm{E}\{x_k^2\}=1/2$, $\mathrm{var}\{x_k^2\}=1/8$, $\mathrm{E}\{x_k^4\}=3/8$. We can assume that the channel has the unit power spectral density (PSD), which means that $\mathrm{E}\{|H_k|^2\}=1$.

Then for the slow and i.i.d. FSF channel with the unit PSD, the subchannels are i.i.d., i.e., H_k is i.i.d. According to Eq. (16), the BER can be represented by

$$\begin{aligned}BER_{i.i.d.}&=\frac{1}{2}\mathrm{erfc}\left[\left(\frac{2\mathrm{var}\{Z_n|(s_n=\pm1)\}}{\mathrm{E}\{Z_n|(s_n=\pm1)\}^2}\right)^{-\frac{1}{2}}\right]\\&=\frac{1}{2}\mathrm{erfc}\left[\left(\frac{2\sum_{w=1}^{3}\mathrm{var}\{P_w|(s_n=\pm1)\}}{\sum_{w=1}^{3}\mathrm{E}\{P_w|(s_n=\pm1)\}}\right)^{-\frac{1}{2}}\right]\\&=\frac{1}{2}\mathrm{erfc}\Bigg[\Bigg(\frac{2\beta\left(\mathrm{E}\left\{|H_k|^4\right\}-1\right)\mathrm{E}\left\{x_k^4\right\}}{\beta^2\mathrm{E}\left\{x_k^2\right\}^2}\\&\quad+\frac{2\beta\left(\mathrm{var}\left\{x_k^2\right\}+N_0^2/2+\mathrm{E}\left\{x_k^2\right\}N_0\right)}{\beta^2\mathrm{E}\left\{x_k^2\right\}^2}\Bigg)^{-\frac{1}{2}}\Bigg]\\&=\frac{1}{2}\mathrm{erfc}\Bigg[\Bigg(\underbrace{\frac{3\left(\mathrm{E}\left\{|H_k|^4\right\}-1\right)}{\beta}}_{(\Delta\Gamma_0)^{-1}}\\&\quad+\underbrace{\frac{1}{\beta}+\frac{2NN_0}{E_b(N-1)}+\frac{N^2N_0^2\beta}{E_b^2(N-1)^2}}_{\Gamma_0^{-1}}\Bigg)^{-\frac{1}{2}}\Bigg]\end{aligned}\tag{17}$$

where $E_b=N\beta\mathrm{E}\{x_k^2\}/(N-1)$ is the average bit energy. Namely, in this case, when β is large enough, $(\Delta\Gamma_0)^{-1}\ll(\Gamma_0)^{-1}$ thus $(\Delta\Gamma_0)^{-1}$ can be omitted, and the statistical distribution of i.i.d. FSF channel will have no influence on BER performances.

Furthermore, for the slow and flat fading channel, the CFR H_k no longer varies with the subcarrier index k. Let H denote this invariant value in one OFDM-DCSK symbol duration, then we have $H_k=H$. Thus the instantaneous BER over the slow flat fading channel can be derived based on Eq. (15) and Eq. (16) as [38], [39]

$$\begin{aligned}&BER(\gamma)\\&=\frac{1}{2}\mathrm{erfc}\left[\left(\frac{1}{\beta}+\frac{2}{\gamma}+\frac{\beta}{\gamma^2}\right)^{-\frac{1}{2}}\right]\\&=\frac{1}{2}\mathrm{erfc}\left[\left(\frac{1}{\beta}+\frac{2NN_0}{|H|^2E_b(N-1)}+\frac{N^2N_0^2\beta}{|H|^4E_b^2(N-1)^2}\right)^{-\frac{1}{2}}\right]\end{aligned}\tag{18}$$

where $\gamma=|H|^2E_b(N-1)/(NN_0)$ and γ is non-negative. Since the instantaneous BER can be represented as the function of γ, as a result, the average BER over the slow flat fading channel can be obtained by calculating the expectation of $BER(\gamma)$, namely we have [39]

$$\begin{aligned}\overline{BER}_{flat}&=\int_0^\infty BER(\gamma)f(\gamma)\mathrm{d}\gamma\\&=\int_0^\infty\frac{1}{2}\mathrm{erfc}\left[\left(\frac{1}{\beta}+\frac{2}{\gamma}+\frac{\beta}{\gamma^2}\right)^{-\frac{1}{2}}\right]f(\gamma)\mathrm{d}\gamma\end{aligned}\tag{19}$$

where $f(\gamma)$ defines the probability distribution function (PDF) of γ. For slow flat fading channel, $f(\gamma)=(e^{-\gamma/\mathrm{E}\{\gamma\}})/\mathrm{E}\{\gamma\}$ [39] and $\mathrm{E}\{\gamma\}=E_b(N-1)/(NN_0)$.

In the special case of AWGN channel, we have $H_k=H=1$, then similar to Eq. (18), the BER can be derived as

$$\begin{aligned}&BER_{AWGN}\\&=\frac{1}{2}\mathrm{erfc}\left[\left(\Gamma_0^{-1}\right)^{-\frac{1}{2}}\right]\\&=\frac{1}{2}\mathrm{erfc}\left[\left(\frac{1}{\beta}+\frac{2NN_0}{E_b(N-1)}+\frac{N^2N_0^2\beta}{E_b^2(N-1)^2}\right)^{-\frac{1}{2}}\right].\end{aligned}\tag{20}$$

Comparing Eq. (17) with Eq. (20), we can observe that when β is large enough, the BER performances of the proposed system over i.i.d. FSF channel with the unit PSD are similar to those over AWGN channel, which will be further verified by simulation results given in Section IV.

2) BER for Eavesdroppers: As mentioned above, the eavesdroppers may not learn the hopping pattern. We here assume that the eavesdroppers use the matrix $\mathbf{X}$ to perform the de-hopping operation to retrieve the information. Then after the OFDM demodulation and the de-hopping, the demodulated data can be obtained as

$$\hat{\mathbf{Z}}=[\hat{\mathbf{z}}_\mathbf{0}^T,\hat{\mathbf{z}}_\mathbf{1}^T,\ldots,\hat{\mathbf{z}}_\mathbf{n}^T,\ldots,\hat{\mathbf{z}}_\mathbf{N-1}^T]^T=(\mathbf{D}'\mathbf{X})^T\tag{21}$$

where $\mathbf{D}'$ denotes the chaotic vector as mentioned in Section II, $\hat{\mathbf{z}}_\mathbf{n}^T$ refers to the nth row of the matrix $\hat{\mathbf{Z}}$.

Thus we can derive the BER of eavesdroppers as [35]

$$BER_{eavesdroppers} = Q\left(\sqrt{\frac{2N \cdot \mathrm{E}[|\mathrm{conj}(\hat{\mathbf{z}}_\mathbf{0})\hat{\mathbf{z}}_\mathbf{n}^T|]}{N_0}}\right). \quad (22)$$

The BER of legitimate receivers can also be expressed in the similar form as

$$BER_{legitimate} = Q\left(\sqrt{\frac{2N \cdot \mathrm{E}[|\mathrm{conj}(\mathbf{d_0})\mathbf{d_n}^T|]}{N_0}}\right) \quad (23)$$

where $\mathbf{D}'$ is replaced with the matrix $\mathbf{D} = [\mathbf{d_0}^T, \mathbf{d_1}^T, \ldots, \mathbf{d_n}^T, \ldots, \mathbf{d_{N-1}}^T]^T$ with the known de-hopping pattern.

C. Security Performance

We then analyze the security performance by calculating the information leakage due to eavesdropping.

Assuming that 0 and 1 are equally probable for transmission, the mutual information between the transmitted data X and the data Y_E recovered by eavesdroppers is [40]

$$\begin{aligned} I_n(Y_E; X) &= H_n(Y_E) - H_n(Y_E|X) \\ &= 1 + p_n \log_2 p_n + (1-p_n)\log_2(1-p_n) \end{aligned} \quad (24)$$

where $H_n(\cdot)$ indicates the entropy operation and p_n is the BER of the eavesdropping receivers at each subcarrier of the FH-OFDM-DCSK system given by Eq. (16).

Assuming the N FH-OFDM-DCSK subcarriers are independent, the information leakage can be derived by [40]

$$L = \frac{1}{N}\sum_{n=0}^{N-1} I_n(Y_E; X). \quad (25)$$

Furthermore, we can derive the secrecy capacity of legitimate users, which represents the secured information rate, as

$$C_{secrecy} = \frac{1}{N}\sum_{n=0}^{N-1} I_n(Y_B; X) - L \quad (26)$$

where $I_n(Y_B; X) = H_n(Y_B) - H_n(Y_B|X) = 1 + p_b \log_2 p_b + (1-p_b)\log_2(1-p_b)$ evaluates the mutual information between the transmitted data X and the received data Y_B, and p_b is the BER of legitimate users.

Notably, since the hopping pattern is non-periodic and can be dynamically updated, it becomes very difficult for eavesdroppers to track and obtain the hopping matrix $\mathbf{U_k}$ in real-time, especially when they use time-consuming brute force cracking methods. For those eavesdroppers who may be unlikely lucky to know that the hopping pattern is cyclic, they have to traverse all possible combinations of $\mathbf{U_k}$, which requires a computation complexity at an order of $O(N!)$. Thus with our design, the information can hardly be retrieved in real time for most practical systems, hence the security performance can be enhanced.

TABLE I
THE COMPLEXITY COMPARISON

System	Complexity
FDE-OFDM-DCSK [9][25]	$O(\beta N \log_2 N)$
FH-OFDM-DCSK	$O(\beta N \log_2 N)$
OFDM-CS-DCSK [32]	$O(\beta N^2) + O(\beta N \log_2(\beta N))$

D. Complexity Analysis

Finally, we analyze and compare the complexity of the proposed FH-OFDM-DCSK system with that of the FDE-OFDM-DCSK system [9], [25] and the OFDM-CS-DCSK system [24]. From Table I, we can observe that the complexity of the proposed FH-OFDM-DCSK system and the FDE-OFDM-DCSK system [9], [25] is lower than that of the OFDM-CS-DCSK system [24].

Specifically, for FDE-OFDM-DCSK system [9], [25], N multiplications are carried out to perform the FDE, while in order to generate an OFDM-DCSK symbol, β times IFFT is required to be carried out, thus the complexity is $O(\beta N \log_2 N)$.

As for the proposed FH-OFDM-DCSK system, the generation of the cyclic hopping pattern has the complexity of $O(N \log_2 N)$, while the hopping process can be regarded as β times matrix multiplication of the N-length vector and the hopping pattern matrix with N non-zero elements sparsely distributed in distinct rows and columns. For this sparse hopping pattern matrix, the wide distribution of element valued "0" will greatly reduce the matrix multiplication complexity, thus for one OFDM-DCSK symbol, only βN scalar multiplications are performed, hence the complexity of the frequency hopping is $O(\beta N)$. Similarly, the de-hopping process also has the complexity of $O(\beta N)$. Since the complexity of the hopping process is much lower than the complexity of the OFDM-DCSK modulation, thus the complexity of the FH-OFDM-DCSK system can be approximately regarded as $O(\beta N \log_2 N)$.

For the OFDM-CS-DCSK system, the complexity of Walsh code spreading is $O(\beta N^2)$ and the complexity of the OFDM modulation for the βN-length vector is $O(\beta N \log_2(\beta N))$, thus the complexity can be obtained as $O(\beta N^2) + O(\beta N \log_2(\beta N))$.

IV. SIMULATION RESULTS

In this section, simulations on BER performance and security performance are provided. Besides, we will compare the performances of FH-OFDM-DCSK systems with the benchmark scheme. Similarly, we also select the FDE-OFDM-DCSK [9], [25] and the OFDM-CS-DCSK [24] systems as benchmark schemes.

A. BER Performance

Firstly, in Fig. 4(a), we demonstrate that the theoretical BER matches the simulated BER performance of the legitimate FH-OFDM-DCSK systems over i.i.d. frequency selective

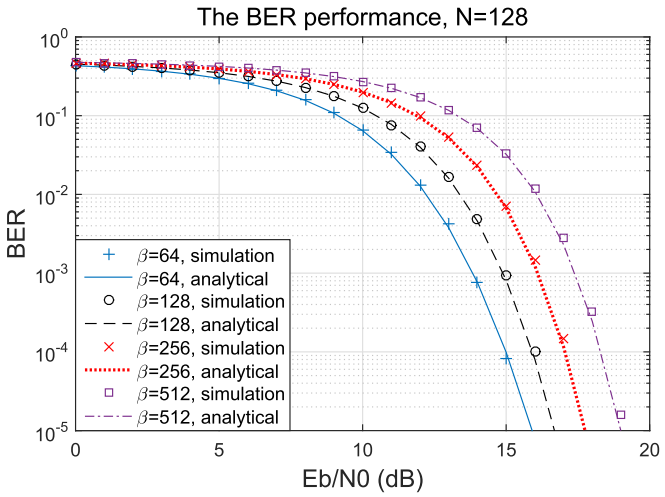

(a) N = 128.

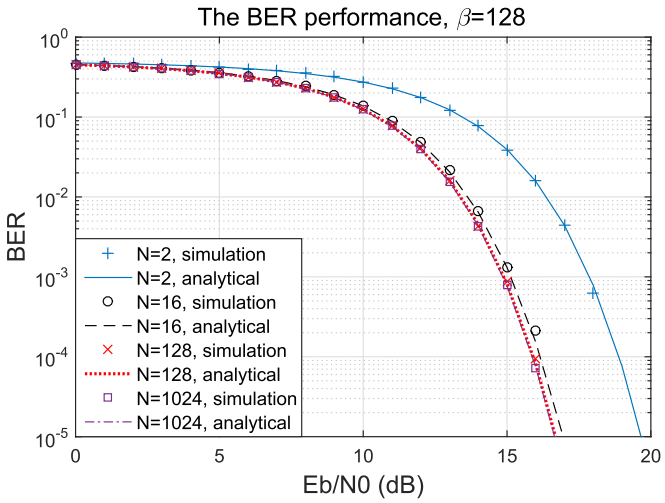

(b) β = 128.

Fig. 4. The theoretical and simulated BER performances of FH-OFDM-DCSK systems over i.i.d. frequency selective Rayleigh fading channel.

Rayleigh fading channel when $\beta = 64, 128, 256, 512$, which verifies the effectiveness of our derivations.

Secondly, Fig. 4(b) also verifies that the effectiveness of our derivations. Besides, it can be observed from Fig. 4(a) and Fig. 4(b) that the BER performances of legitimate FH-OFDM-DCSK systems become better for larger subcarrier number N and smaller chaotic sequence length $\beta = 128$. When N is larger than 16, the BER performances are weakly related to N, which is in accordance with the theoretical result given by Eq. (16) that the value of the fraction $N/(N-1)$ is close to 1. Moreover, as mentioned above, since the i.i.d. FSF channel can be seen as the multipath channel having infinite channel paths, thus thanks to the FH operation, the FH-OFDM-DCSK system can achieve full frequency diversity gain, which will lead to outstanding BER performances to be further illustrated in the following results.

Then we investigate the influence of hopping pattern on BER performance in Fig. 5, where the pre-defined pattern represents that the hopping pattern remains unchanged during the transmissions of the information symbols, while the random

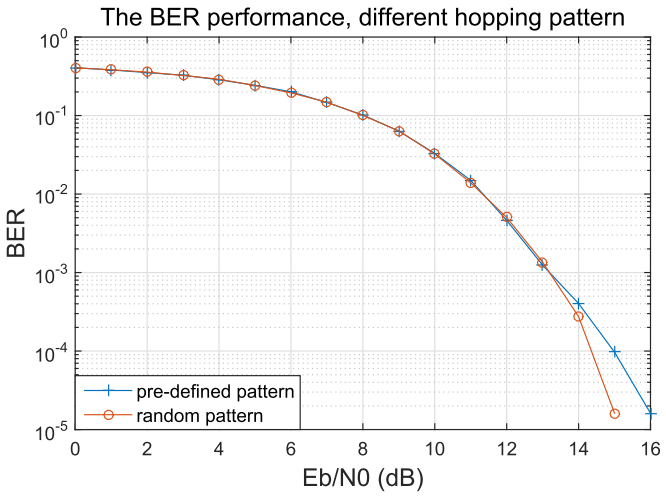

Fig. 5. The BER performances of FH-OFDM-DCSK systems over i.i.d. frequency selective Rayleigh fading channel when difference hopping pattern is employed.

hopping pattern means that every FH-OFDM-DCSK symbol hops with different hopping patterns. It can be observed that the BER performances are almost unrelated with the hopping pattern settings. The variations of the hopping pattern among each transmitted symbol will not affect the BER performance, but will bring the benefit of enhanced security performance since it is more difficult for eavesdroppers to learn the hopping pattern.

B. Robustness Performance

In order to demonstrate the robustness performance of our design, we compare the BER performances of the proposed FH-OFDM-DCSK scheme with those of benchmark schemes over FSF channels with imperfect CSI or unknown CSI. As mentioned above, for fairness of comparisons, we propose to add the FDE module to the OFDM-DCSK receiver to combat the fading. Additionally, the same parameter settings are employed in the systems used for comparisons.

1) CCDF Performance Comparison: In Fig. 6, we firstly compare the correlations among the OFDM symbols between the proposed FH-OFDM-DCSK system and the FDE-OFDM-DCSK [9], [25]. Here we evaluate the correlations with $C_{j,k} = \Re\left\{\sum_{i=0}^{N-1} \mathrm{conj}(r_{i,j}) \cdot r_{i,k}\right\}$, where $r_{i,j}$ is the ith chip of the jth received OFDM symbol and $r_{i,k}$ is the ith chip of the kth OFDM symbol. Furthermore, we define a complementary cumulative distribution function (CCDF) of $C_{j,k}$ as

$$CCDF(C_0) = Pr(C_{j,k} > C_0) \tag{27}$$

where C_0 is the correlation threshold and $Pr(C_{j,k} > C_0)$ denotes the probability that the correlation value is larger than the correlation threshold.

It can be observed from Fig. 6 that the FH-OFDM-DCSK system achieves a much lower CCDF than the FDE-OFDM-DCSK system, which means that weaker correlations among the information-bearing symbols and more reliable communication performances can be achieved thanks to the frequency hopping.

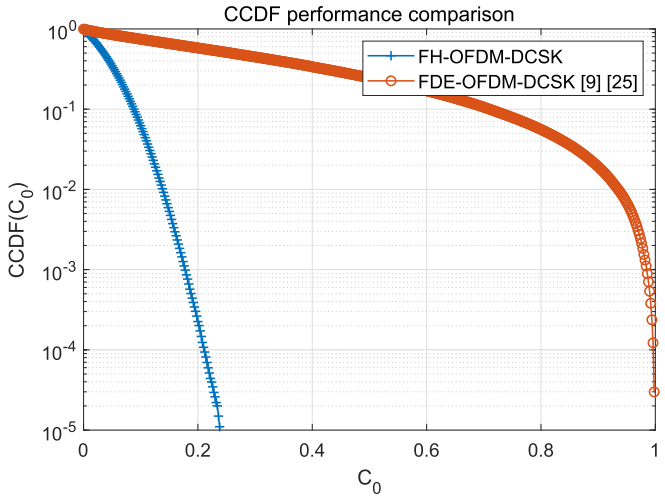

Fig. 6. The CCDF performance comparison between the FH-OFDM-DCSK system and the FDE-OFDM-DCSK system [9], [25] when $N = 128$ and $\beta = 128$.

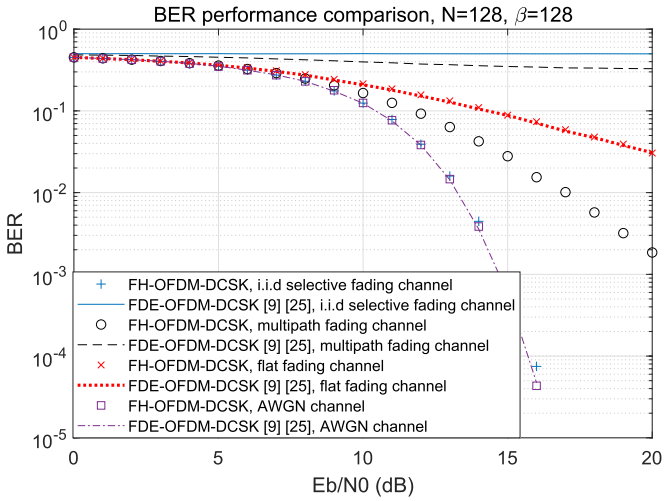

Fig. 7. The BER performance comparison of the FH-OFDM-DCSK system and the FDE-OFDM-DCSK system [9], [25] over different channels without CSI when $N = 128$ and $\beta = 128$.

2) BER Performance Comparison Over Different Channels: In Fig. 7, we investigate the BER performances of the FH-OFDM-DCSK and FDE-OFDM-DCSK systems over the following four types of channels without CSI:

- i.i.d. Rayleigh FSF channel with $\mathrm{E}\{|H_k|^2\} = 1$;
- multipath FSF channel with the model $r_{i,k} = \sum_{l=1}^{P_L} h_l \, s_{((i-l))_N,k} + \xi_{i,k}$ where the number of paths P_L is 3, $((\cdot))_N$ denotes the cyclic shift in the base of N, each path has the average power of $\mathrm{E}\{|h_l|^2\} = 1/3$ and $\xi_{i,k}$ is the Gaussian noise having the power of N_0;
- slow flat fading channel;
- AWGN channel.

We can see from Fig. 7 that the proposed system has achieved the best BER performances over i.i.d. FSF channel, which outperforms the BER performances of the FDE-OFDM-DCSK system significantly and approach those over AWGN channel. The observations match the conclusion drawn from Eq. (17) and Eq. (20) that the BER performances over these 2 channels are similar when β is large enough. In the case of transmitting signals over multipath FSF channel, BER performances of the proposed system is worse than those over i.i.d. frequency selective Rayleigh fading channel, but still outperform BER performances of FDE-OFDM-DCSK systems. The reason is that H_k is correlated with each other when the FSF is induced by multipath propagations, which decreases the frequency diversity gain and BER performances become worse. Moreover, in the scenarios that the signals are transmitted over slow flat fading channel and AWGN channel, the proposed system attains the same BER performances as those of FDE-OFDM-DCSK systems, since no frequency diversity can be utilized. The lack of frequency diversity also incurs that the BER performances of the proposed system over slow flat fading channel become worse than those over multipath Rayleigh fading channel and i.i.d. FSF channel.

3) BER Performance Comparison for Imperfect CSI: In order to investigate the effects of imperfect CSI on the performances of multicarrier transmission systems, next we compare the BER performances of the FH-OFDM-DCSK systems with benchmark schemes over FSF channels.

The imperfect CSI is obtained via the channel estimation module given by [41], [42]

$$\hat{H}_{n,k} = \rho H_{n,k} + \sqrt{1-\rho^2}\epsilon_{n,k} \tag{28}$$

where $\hat{H}_{n,k}$ is the estimated CFR, $H_{n,k}$ is the actual CFR with zero mean and unit power spectral density, the estimation error $\epsilon_{n,k}$ is a Gaussian random variable independent from $H_{n,k}$ and has 0 mean and the variance of σ_e^2 which equals to the power of errors, and the correlation coefficient ρ determines the quality of channel estimations.

In Fig. 8, we compare the BER performances of the proposed FH-OFDM-DCSK system and the FDE aided OFDM-DCSK system [9], [25] over i.i.d. FSF channel. Notably, in order to combat the fading, FDE module is added to the OFDM-DCSK system to compensate the CFR which will induce the phase rotations of symbols thereby degrading the detection performances. Thus the exact CSI is required because the erroneous CSI might also induce performance degradations.

Fig. 8(a) and Fig. 8(b) respectively demonstrate the performances when ρ and σ_e^2 of CSI are different. It can be observed that thanks to the frequency diversity gain, the proposed FH-OFDM-DCSK system achieves better performances than the FDE-OFDM-DCSK system no matter whether exact CSI can be obtained or not.

Besides, we can notice from Fig. 8(a) that with the aid of the FDE module and exact CSI, i.e. $\rho = 1$, the BER performances of FDE-OFDM-DCSK systems [9] [25] are improved and better than those attained with lower CSI estimation accuracy when $\rho = 0.7$. Moreover, for larger power of CSI estimation error corresponding to $\sigma_e^2 = 0.6$, we can observe from Fig. 8(b) that the BER performances of the FDE-OFDM-DCSK system are worse than those achieved when $\sigma_e^2 = 0$. By contrast, thanks to the frequency diversity gain, the CSI estimation errors induced by lower ρ or higher σ_e^2 have few impacts on the proposed FH-OFDM-DCSK design.

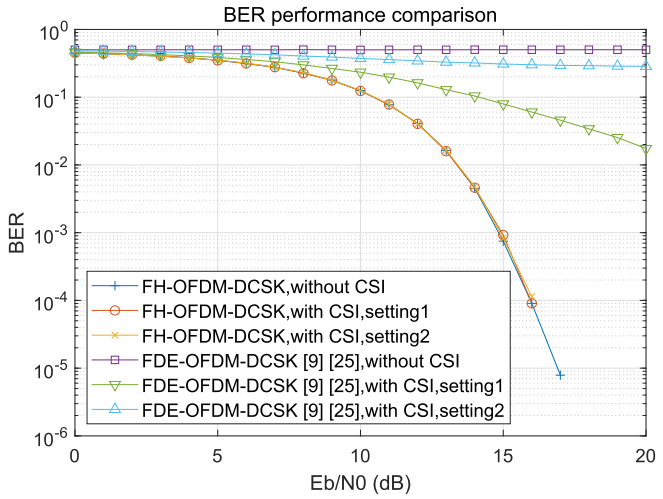

(a) BER performances with different ρ. (setting1: $\sigma_e^2 = 1$, $\rho = 1$, setting2: $\sigma_e^2 = 1$, $\rho = 0.7$)

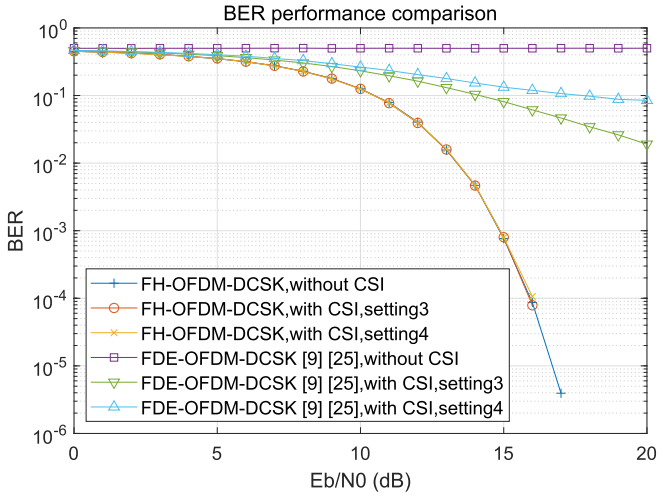

(b) BER performances with different σ_e^2. (setting3: $\sigma_e^2 = 0$, $\rho = 0.9$, setting4: $\sigma_e^2 = 0.6$, $\rho = 0.9$)

Fig. 8. The BER performance comparison of the FH-OFDM-DCSK system and the FDE-OFDM-DCSK system [9], [25] over i.i.d. FSF channel when $N = 128$ and $\beta = 128$.

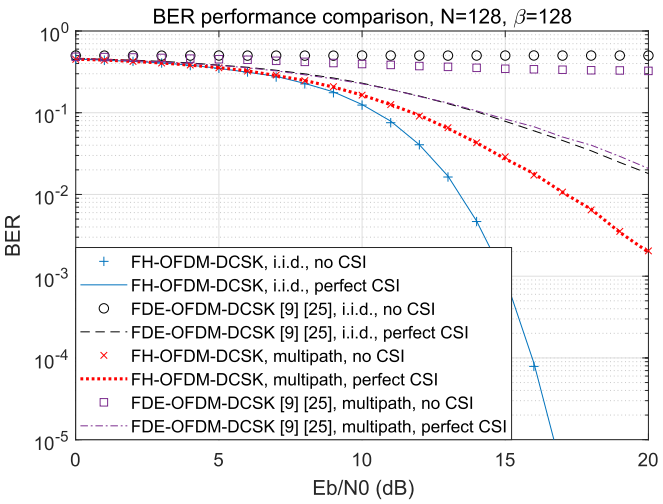

Fig. 9. The BER performance comparison of the FH-OFDM-DCSK system and the FDE-OFDM-DCSK system [9], [25] over i.i.d. FSF and multipath FSF channels with and without CSI estimation when $N = 128$ and $\beta = 128$.

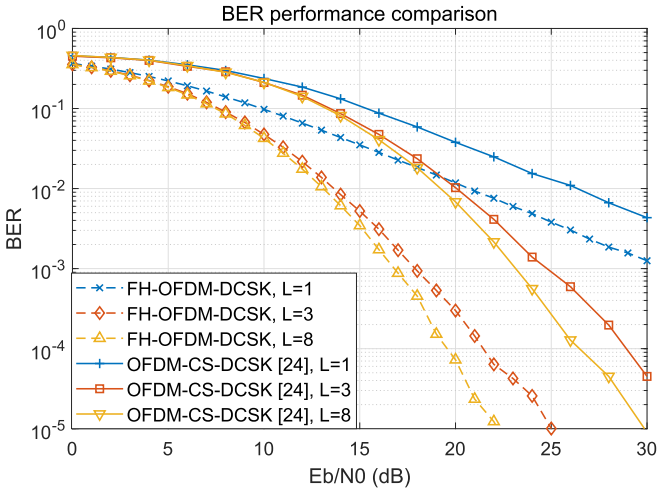

Fig. 10. The BER performance comparison of the FH-OFDM-DCSK system and the OFDM-CS-DCSK system [24] over multi path FSF channels when $N\beta = 64$.

Therefore, the proposed FH-OFDM-DCSK system can achieve more robust and reliable performances than the benchmark scheme when CSI estimates are imperfect.

Subsequently, we investigate the BER performances over i.i.d. FSF channel and multipath FSF channel. As illustrated by Fig. 9, similar to the observations in Fig. 8, the proposed system can attain almost the same BER performances no matter whether exact CSI can be obtained or not, which again validate the robustness and high reliability performances of our design.

Moreover, we compare the BER performances of the FH-OFDM-DCSK system with the OFDM-CS-DCSK system [24], which can defend against the FSF over multipath FSF channels, where P_L denotes the channel path number. In the simulation, each channel path has the average power of $\mathrm{E}\{(h_l^2)\} = \mathrm{E}\{(h_1^2)\}e^{-\epsilon(l-1)}$ for $l = 1, 2, \ldots, P_L$, the power decay factor of $\epsilon = 1$ and the summed average power of $\sum_{l=1}^{P_L} \mathrm{E}\{(h_l^2)\} = 1$ [24]. The length of CP is 8.

It can be seen from Fig. 10 that the proposed FH-OFDM-DCSK system achieves better BER performances over frequency selective Rayleigh fading channels. When the number of paths increases, better BER performances can be achieved since more frequency diversity gain can be utilized. As mentioned previously, for i.i.d. FSF channels, full frequency diversity gain can be utilized, thus the BER performances of the FH-OFDM-DCSK system will approach those over AWGN channel. Moreover, the FH-OFDM-DCSK system can always attain better BER performances than the counterpart OFDM-CS-DCSK systems thanks to the diversity provided by the frequency hopping.

C. Security Performance

Fig. 11(a) compares the BER performances of legitimate receivers and eavesdroppers. Since the frequency hopping pattern is known for legitimate users, lower BER and reliable

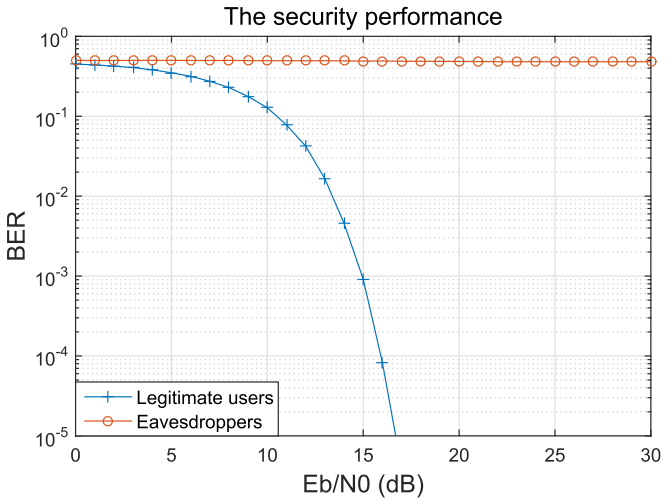

(a) BER performances of legitimate users and eavesdroppers.

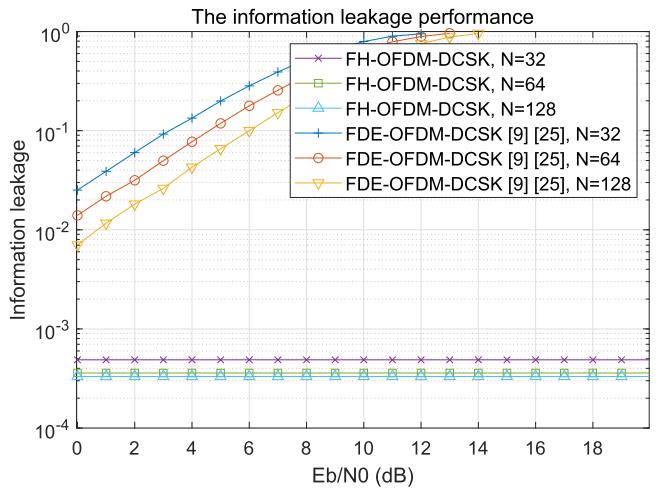

(b) Information leakage comparison.

Fig. 11. The security performance demonstrations and comparisons of the FH-OFDM-DCSK system and the FDE-OFDM-DCSK system [9], [25] when $N = 128$ and $\beta = 128$.

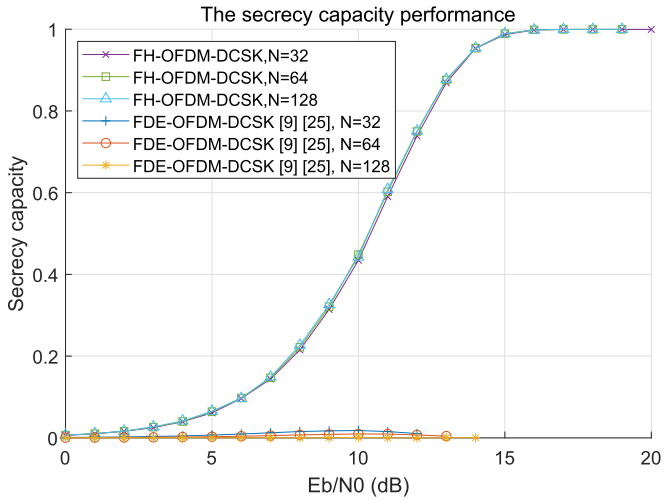

Fig. 12. The secured information rate comparison between the FH-OFDM-DCSK system and the FDE-OFDM-DCSK system [9], [25].

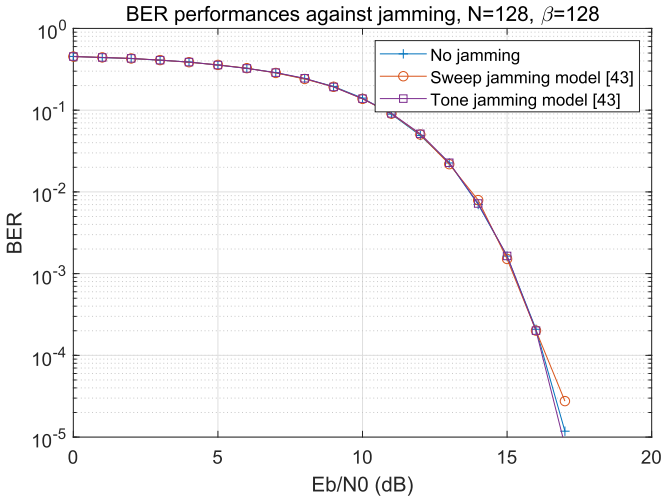

Fig. 13. BER performances of the FH-OFDM-DCSK system against jamming, $N = 128$, $\beta = 128$.

performances can be achieved. By contrast, eavesdroppers can hardly learn the correct hopping pattern, hence with the wrong hopping pattern, they could not retrieve the information due to the high BER.

Moreover, Fig. 11(b) illustrates the information leakage rate for eavesdropping in the FH-OFDM-DCSK system and FDE-OFDM-DCSK system [9], [25] using Eq. (24) and Eq. (25). It can be seen from the figure that thanks to the frequency hopping, in the FH-OFDM-DCSK systems, eavesdroppers can hardly recover the transmitted information from the intercepted data, and the information leakage performances are much better than those of FDE-OFDM-DCSK systems. It is also noticeable that in FDE-OFDM-DCSK systems, when E_b/N_0 and the subcarrier number is large enough, eavesdroppers can retrieve the data and the information leakage rate is close to 1, while our proposed FH-OFDM-DCSK can always provide secure communication services with low information leakage rate.

To elaborate a bit further, we compare the secrecy capacity performance of the FH-OFDM-DCSK system with the benchmark FDE-OFDM-DCSK system [9], [25] as illustrated in Fig. 12. It can be seen from the figure that the FH-OFDM-DCSK system obviously achieves much higher secured data rate than the benchmark FDE-OFDM-DCSK system [9], [25] whose secured information rate approaches to 0. The reason is that in FDE-OFDM-DCSK systems, the reference chaotic signal is transmitted directly over specific subcarriers, thus eavesdroppers can easily retrieve the information and no security can be guaranteed for the information transmissions. By contrast, in our design, thanks to the frequency hopping, the malicious users cannot retrieve the information without the known frequency hopping pattern in real time due to the high complexity of brute forcing attacks. Hence we could draw a conclusion that the proposed FH-OFDM-DCSK system can effectively improve the security performance and increase the secured information rate.

D. Anti-Jamming Performance

Finally, Fig. 13 demonstrates the anti-jamming capability of the proposed FH-OFDM-DCSK system in terms of BER

performances. Here we use the jamming model given in [43], wherein the ith jamming chip of the sweep jamming model is denoted as $\sqrt{2P_j}\sin\left(2\pi i F_{start}/N + \pi i^2 \Delta F/N^2\right)$ and the ith jamming chip of the tone jamming model is denoted as $\sum_{m_j=1}^{M_j}\sqrt{2P_j/M_j}\sin\left(\pi i F_m/N\right)$ where P_j denotes the power of the jamming signal, the range of i is $0 \le i \le N-1$, F_{start} is set as 1, ΔF is set as 4, $M_j = 4$ is the number of tones, F_m is set as $[1, 3, 5, 7]$. Moreover, we assume that the cycle of the jamming signal is the duration of one OFDM symbol and the information is transmitted over i.i.d. FSF channel.

We can see from Fig. 13 that the proposed FH-OFDM-DCSK system can achieve similar BER performances compared with the one without jamming. The reason is given as follows. The jamming can be viewed as the sine wave added to the desired signal in the time domain. At the receiver, the FFT will transform the jamming signal from the sine wave to a high-power signal in a narrow band. In our design, thanks to the FH operation, this high-power signal will appear over specific subcarriers and only the chaotic chips from the same index of every chaotic sequence are polluted, which enables the FH-OFDM-DCSK receiver to be capable of anti-jamming since few polluted chaotic chips from all chaotic sequences with the high power and the same index are thrown away. For example, as shown in Fig. 13, if we use the unpolluted 113 chips from $\beta = 128$ chips to perform the correlation demodulation, the FH-OFDM-DCSK achieves similar BER performances to those when no jamming exists, which demonstrates the anti-jamming capability of our design.

V. Conclusion

In this paper, we propose a frequency hopping OFDM-DCSK scheme to enhance both reliability and robustness performances. By exploiting the frequency diversity provided by the frequency hopping, the chips from all chaotic sequences hop non-repetitively and are transmitted over different subcarriers in different time slots. Thus the CFR of each subchannel is naturally embedded into the chaotic chips and will be used for information recovery in the receivers. Hence the requirement for exact CSI is removed, and the proposed FH-OFDM-DCSK scheme can be used for practical communication systems with unknown CSI or imperfect CSI. Furthermore, we analyze the energy efficiency and spectral efficiency, derive BER and information leakage expressions and provide the complexity analysis, then numerical simulations are provided to verify the effectiveness of our theoretical analysis. Simulation results under different parameter settings demonstrate that the proposed FH-OFDM-DCSK systems can achieve better BER and security performances than counterpart schemes over FSF channels, thereby better reliability, security and robustness performances can be achieved by applying our design. Therefore, the proposed FH-OFDM-DCSK design can effectively enable high data rate CA or CR systems to provide more reliable and secure transmission services over contiguous or non-contiguous bands without requiring CSI.

References

[1] A. Ghosh, R. Ratasuk, B. Mondal, N. Mangalvedhe, and T. Thomas, "LTE-advanced: Next-generation wireless broadband technology [invited paper]," *IEEE Wireless Commun.*, vol. 17, no. 3, pp. 10–22, Jun. 2010.

[2] D. Cabrić, S. M. Mishra, D. Willkomm, R. Brodersen, and A. Wolisz, "A cognitive radio approach for usage of virtual unlicensed spectrum," in *Proc. 14th IST Mobile Wireless Commun. Summit*, Dresden, Germany, Jun. 2005.

[3] Y. Fang, G. Han, P. Chen, F. C. M. Lau, G. Chen, and L. Wang, "A survey on DCSK-based communication systems and their application to UWB scenarios," *IEEE Commun. Surveys Tuts.*, vol. 18, no. 3, pp. 1804–1837, 3rd Quart., 2016.

[4] G. Kaddoum and N. Tadayon, "Differential chaos shift keying: A robust modulation scheme for power-line communications," *IEEE Trans. Circuits Syst. II, Exp. Briefs*, vol. 64, no. 1, pp. 31–35, Jan. 2017.

[5] F. C. M. Lau and C. K. Tse, *Chaos-Based Digital Communication Systems*. New York, NY, USA: Springer, 2003.

[6] G. Kolumbán, B. Vizvári, W. Schwarz, and A. Abel, "Differential chaos shift keying: A robust coding for chaos communication," in *Proc. NDES*, 1996, pp. 87–92.

[7] M. Dawa, G. Kaddoum, and Z. Sattar, "A generalized lower bound on the bit error rate of DCSK systems over multi-path Rayleigh fading channels," *IEEE Trans. Circuits Syst. II, Exp. Briefs*, vol. 65, no. 3, pp. 321–325, Mar. 2018.

[8] G. Kaddoum, F. Richardson, and F. Gagnon, "Design and analysis of a multi-carrier differential chaos shift keying communication system," *IEEE Trans. Commun.*, vol. 61, no. 8, pp. 3281–3291, Aug. 2013.

[9] S. Li, Y. Zhao, and Z. Wu, "Design and analysis of an OFDM-based differential chaos shift keying communication system," *J. Commun.*, vol. 10, no. 3, pp. 199–205, 2015.

[10] G. Kaddoum, "Design and performance analysis of a multiuser OFDM based differential chaos shift keying communication system," *IEEE Trans. Commun.*, vol. 64, no. 1, pp. 249–260, Jan. 2016.

[11] Z. Galias and G. M. Maggio, "Quadrature chaos-shift keying: Theory and performance analysis," *IEEE Trans. Circuits Syst. I, Fundam. Theory Appl.*, vol. 48, no. 12, pp. 1510–1519, Dec. 2001.

[12] H. Yang and G.-P. Jiang, "High-efficiency differential-chaos-shift-keying scheme for chaos-based noncoherent communication," *IEEE Trans. Circuits Syst. II, Exp. Briefs*, vol. 59, no. 5, pp. 312–316, May 2012.

[13] F. Taleb, F. T. Bendimerad, and D. Roviras, "Very high efficiency differential chaos shift keying system," *IET Commun.*, vol. 10, no. 17, pp. 2300–2307, Nov. 2016.

[14] H. Yang and G.-P. Jiang, "Reference-modulated DCSK: A novel chaotic communication scheme," *IEEE Trans. Circuits Syst. II, Exp. Briefs*, vol. 60, no. 4, pp. 232–236, Apr. 2013.

[15] H. Yang, G. Jiang, L. Xia, and X. Tu, "Reference-shifted DCSK modulation scheme for secure communication," in *Proc. Int. Conf. Comput., Netw. Commun. (ICNC)*, Jan. 2017, pp. 1073–1076.

[16] G. Kaddoum, E. Soujeri, C. Arcila, and K. Eshteiwi, "I-DCSK: An improved noncoherent communication system architecture," *IEEE Trans. Circuits Syst. II, Exp. Briefs*, vol. 62, no. 9, pp. 901–905, Sep. 2015.

[17] G. Kaddoum, E. Soujeri, and Y. Nijsure, "Design of a short reference noncoherent chaos-based communication systems," *IEEE Trans. Commun.*, vol. 64, no. 2, pp. 680–689, Jan. 2016.

[18] M. Herceg, D. Vranješ, G. Kaddoum, and E. Soujeri, "Commutation code index DCSK modulation technique for high-data-rate communication systems," *IEEE Trans. Circuits Syst. II, Exp. Briefs*, vol. 65, no. 12, pp. 1954–1958, Dec. 2018.

[19] W. Hu, L. Wang, and G. Kaddoum, "Design and performance analysis of a differentially spatial modulated chaos shift keying modulation system," *IEEE Trans. Circuits Syst. II, Exp. Briefs*, vol. 64, no. 11, pp. 1302–1306, Nov. 2017.

[20] W. Hu, L. Wang, G. Cai, and G. Chen, "Non-coherent capacity of M-ary DCSK modulation system over multipath Rayleigh fading channels," *IEEE Access*, vol. 5, pp. 956–966, 2017.

[21] A. Kumar, P. R. Sahu, and J. Mishra, "Performance analysis of DCSK modulation with diversity combining not requiring channel state information," in *Proc. 22nd Nat. Conf. Commun. (NCC)*, Mar. 2016, pp. 1–6.

[22] S. Wang and X. Wang, "M-DCSK-Based chaotic communications in MIMO multipath channels with no channel state information," *IEEE Trans. Circuits Syst.-II*, vol. 57, no. 12, pp. 1001–1005, Dec. 2010.

[23] P. Chen, L. Wang, and F. C. M. Lau, "One analog STBC-DCSK transmission scheme not requiring channel state information," *IEEE Trans. Circuits Syst. I, Reg. Papers*, vol. 60, no. 4, pp. 1027–1037, Apr. 2013.

[24] M. Chen, W. Xu, D. Wang, and L. Wang, "Design of a multi-carrier different chaos shift keying communication system in doubly selective fading channels," in *Proc. 23rd Asia–Pacific Conf. Commun. (APCC)*, Dec. 2017, pp. 1–6.
[25] X. Ouyang and J. Zhao, "Single-tap equalization for fast OFDM signals under generic linear channels," *IEEE Commun. Lett.*, vol. 18, no. 8, pp. 1319–1322, Aug. 2014.
[26] H. Schulze and C. Lüders, *Theory and Applications of OFDM and CDMA: Wideband Wireless Communications*. Hoboken, NJ, USA: Wiley, 2005.
[27] G. Kaddoum, "Wireless chaos-based communication systems: A comprehensive survey," *IEEE Access*, vol. 4, pp. 2621–2648, 2016.
[28] F. C. M. Lau, K. Y. Cheong, and C. K. Tse, "Permutation-based DCSK and multiple-access DCSK systems," *IEEE Trans. Circuits Syst. I, Fundam. Theory Appl.*, vol. 50, no. 6, pp. 733–742, Jun. 2003.
[29] M. Herceg, G. Kaddoum, D. Vranješ, and E. Soujeri, "Permutation index DCSK modulation technique for secure multiuser high-data-rate communication systems," *IEEE Trans. Veh. Technol.*, vol. 67, no. 4, pp. 2997–3011, Apr. 2018.
[30] W. Ma, J. Du, and H. Xue, "Design of reverse-DCSK for chaos based communication system," in *Proc. 3rd IEEE Int. Conf. Comput. Commun. (ICCC)*, Dec. 2017, pp. 743–747.
[31] H. Cai, Z. Hua, and H. Huang, "A novel differential-chaos-shift-keying secure communication scheme," in *Proc. IEEE Int. Conf. Syst., Man, Cybern. (SMC)*, Oct. 2018, pp. 1794–1798.
[32] G. Kaddoum, F. Gagnon, and F.-D. Richardson, "Design of a secure multi-carrier DCSK system," in *Proc. 9th Int. Symp. Wireless Commun. Syst. (ISWCS)*, Aug. 2012, pp. 964–968.
[33] S. Zhou, G. B. Giannakis, and A. Scaglione, "Long codes for generalized FH-OFDMA through unknown multipath channels," *IEEE Trans. Commun.*, vol. 49, no. 4, pp. 721–733, Apr. 2001.
[34] T. Scholand *et al.*, "Fast frequency hopping OFDM concept," *Electron. Lett.*, vol. 41, no. 13, pp. 748–749, Jun. 2005.
[35] H. Lu, L. Zhang, M. Jiang, and Z. Wu, "High-security chaotic cognitive radio system with subcarrier shifting," *IEEE Commun. Lett.*, vol. 19, no. 10, pp. 1726–1729, Oct. 2015.
[36] C. Pöpper, M. Strasser, and S. Capkun, "Anti-jamming broadcast communication using uncoordinated spread spectrum techniques," *IEEE J. Sel. Areas Commun.*, vol. 28, no. 5, pp. 703–715, Jun. 2010.
[37] B. Chen, L. Zhang, and H. Lu, "High security differential chaos-based modulation with channel scrambling for WDM-aided VLC system," *IEEE Photon. J.*, vol. 8, no. 5, Oct. 2016, Art. no. 7804513.
[38] Y. Xia, C. K. Tse, and F. C. M. Lau, "Performance of differential chaos-shift-keying digital communication systems over a multipath fading channel with delay spread," *IEEE Trans. Circuits Syst. II, Exp. Briefs*, vol. 51, no. 12, pp. 680–684, Dec. 2004.
[39] Z. Liu, L. Zhang, and Z. Chen, "Low PAPR OFDM-based DCSK design with carrier interferometry spreading codes," *IEEE Commun. Lett.*, vol. 22, no. 8, pp. 1588–1591, Aug. 2018.
[40] H. Li, X. Wang, and Y. Zou, "Dynamic subcarrier coordinate interleaving for eavesdropping prevention in OFDM systems," *IEEE Commun. Lett.*, vol. 18, no. 6, pp. 1059–1062, Jun. 2014.
[41] B. Prasad, S. D. Roy, and S. Kundu, "Outage and SEP of secondary user with imperfect channel estimation and primary user interference," in *Proc. IEEE Int. Conf. Electron., Comput. Commun. Technol. (CONECCT)*, Jan. 2014, pp. 1–6.
[42] A. Pascual-Iserte, D. P. Palomar, A. I. Pérez-Neira, and M. Á. Lagunas, "A robust maximin approach for MIMO communications with imperfect channel state information based on convex optimization," *IEEE Trans. Signal Process.*, vol. 54, no. 1, pp. 346–360, Jan. 2006.
[43] B. Van Nguyen, M. T. Nguyen, H. Jung, and K. Kim, "Designing anti-jamming receivers for NR-DCSK systems utilizing ICA, WPD, and VMD methods," *IEEE Trans. Circuits Syst. II, Exp. Briefs*, vol. 66, no. 9, pp. 1522–1526, Sep. 2019.

Zhaofeng Liu received the B.S. degree in communication engineering from Sun Yat-sen University, Guangzhou, China, in 2017, where he is currently pursuing the master's degree in electronics and communication engineering. His research interests include chaotic communication, multi-carrier communication, cognitive radios, and the Internet of Things.

Lin Zhang (M'16) received the B.S. and M.S. degrees in electrical engineering from Shanghai University in 1997 and 2000, respectively, and the Ph.D. degree in electrical engineering from Sun Yat-sen University in 2003. She joined the Department of Electrical Engineering, Sun Yat-sen University, in 2003, where she has been an Associate Professor since 2007. From 2008 to 2009, she was a Visiting Researcher with the Electrical and Computer Engineering Department, University of Maryland, College Park, USA, for one year. Her research was supported by the National Natural Science Foundation of China and the Science and Technology Program Project of Guangdong Province. Her current research interests include signal processing and their applications to wireless communication systems.

Zhiqiang Wu (M'02–SM'17) received the B.S. degree from the Beijing University of Posts and Telecommunications in 1993, the M.S. degree from Peking University in 1996, and the Ph.D. degree from Colorado State University in 2002, all in electrical engineering. He has also held visiting positions at Peking University, Harbin Engineering University, Guizhou Normal University, and Tibet University. He served as an Assistant Professor with the Department of Electrical and computer Engineering, West Virginia University Institute of Technology, from 2003 to 2005. He joined Wright State University in 2005, where he is currently a Full Professor with the Department of Electrical Engineering. His research was supported by the NSF, AFRL, ONR, AFOSR, and OFRN.

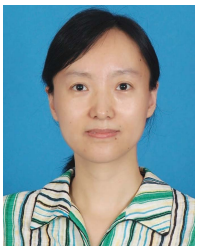

Jing Bian received the B.S. degree in automation, the M.S. degree in computational mathematics, and the Ph.D. degree in electrical engineering from Sun Yat-sen University, in 1988, 2001, and 2006, respectively. She served as an Associate Professor with the School of Mathematics and Computational Science, Sun Yat-sen University, from 1994 to 2015, where she has been an Associate Professor with the School of Data and Computer Science since 2015. Her research interests include blockchain technology and security and wireless communication networks.